

Deep Robotic Grasping Prediction with hierarchical RGB-D Fusion

Yaoxian Song^{1,2}, Jun Wen, Yuejiao Fei¹, Changbin Yu¹

Abstract—Robotic arm grasping is a fundamental operation in robotic control task goals. We consider grasping problem by multimodal hierarchical fusion to generate grasping policy with partial observation. The most of current methods for robotic grasping focus on RGBD policy in table surface scene or 3D point cloud analysis inference in 3D space. Comparing to these methods, we propose a novel multimodal hierarchical deep method that fuses RGB and depth data to realize robotic humanoid grasping in 3D space with only partial observation. Under supervised learning, we develop a general label algorithm to label ground-truth in common RGBD dataset. A real-time hierarchical encoder-decoder neural network is designed to generate grasping policy. We evaluate the effectiveness and performance of our method on a physical robot setup. The results of experiment validate our method. The video is available in https://youtu.be/Wxw_r5a8qV0.

I. INTRODUCTION

Rapid and reliable robotic grasping has been researched for many years which widely applied in manufacturing, medicine, retail and service robots [1]. Picking and transferring a specific object from one place to another place in the unstructured environment is a fundamental operation among tasks of the robotic arm.

Traditional methods to solve the robotic grasping problem estimate the shape and pose of the objects [2] [3]. To solve the robotic grasping problem, it needs to obtain object geometric knowledge, environment configuration and robot setup information together to design the grasping controller. Unfortunately, it is difficult to extract that information precisely. For most scenarios, the object geometric observation is partial and the environment is too complicated to model directly. To relieve these uncertainty problems mentioned above, [4] [5] split the grasping task into several steps in the Amazon Picking Challenge. Firstly, object detection or segmentation are taken from the observation. Then, it fits a 3D model to a segmented point cloud to recover the 6D pose of the object. Motion generation is taken based on the object pose. The deep neural network is adopted to better estimation performance.

Apart from the traditional method, methods based on end-to-end learning are an alternative to achieve more robust and superior performance. Recent work [6] [7] [8] [9] have shown the potential to overcome the challenges in grasping process. [6] explores training a deep neural network from a synthetic dataset to reduce data collection. This work

generates grasping policy in real-time directly. Comparing to [6] obtaining grasping policy by sampling grasping candidates indirectly, [7] predicts the best grasping by an encoder-decoder neural network end-to-end. Furthermore, deep reinforcement learning(RL) method is also applied in the grasping task. They achieve grasping skills by continues interacting with the environment. Most of the existing deep RL works still keep in simple object grasping exploration.

Most state-of-the-art works design their deep neural network including convolutional neural network(CNN) and fully convolutional network(FCN). The inputs of the network are usually proprioception of robot, force, RGB image, depth image or point cloud. And the dataset is absent comparing to typical computer vision problems.

In this paper, we proposed a new method of grasping the target object using multimodal data in the unstructured environment. Our key idea is to formulate the grasping problem as a mapping modeling task from partial observation space of the robot to the grasping space. To solve the task, we design a multimodal fused hierarchical deep neural network to model the mapping relationship. RGB and depth image on an eye-in-hand camera system are fed into the network. our work considers data denoising and uncertainty qualification additionally. Our primary contributions are:

- A novel label algorithm is proposed. We can use common computer vision dataset which need to contain RGB, depth and object mask image to train a grasping neural network without human label.
- A RGBD fused hierarchical encoder-decoder fully convolutional network is proposed to generate grasping policy. Comparing to existing works, we only use partial observation to realize humanoid grasping without iteration close point or object reconstruction, etc.
- We evaluate the effectiveness of our method by designing a grasping pipeline on a physical grasping setup.

II. RELATED WORK

A. Learning based robotic grasping

Robotic grasping or pick-place is a highly fundamental problem which has been researched for decades. Traditional analytic methods concentrate on creating a 3D object models database and register sensor data to known object in the database [10] [11] [12] [13]. These methods do not generalize well in a large variety of novel objects in practice [14]. Learning based methods become popular with the widely adoption of deep learning technic. [15] [16] [17] [7] use deep learning to generate grasping policy. [8] [9] [18] [19] [20] design controller using deep RL by exploring robotic task environment and finally realize robotic grasping.

¹The authors are with School of Engineering at Westlake University Emails: {songyaoxian, feiyuejiao, yuchangbin}@westlake.edu.cn

²The authors are also PhD students in Computer Science at Fudan University.

B. Multimodal perception

Different from other learning-based problem, robotic control with multisensor data fusion has been researched many years in the control field. Robotic sensors usually consist of RGBD camera, inertial measurement unit, laser radar, haptic device, etc. The complementary nature of different sensor modalities has been explored in robotic inference and decision making. [21] adopts RGB and depth image to estimate the surface normal of the object. [6] [16] [22] [23] [24] [25] based on RGB image with depth or point cloud to predict grasping policy. [26] [27] [28] [29] are used to train a grasping network fusing RGB and haptic data. In [30], not only visual and force-torque data is used but the robotic proprioception including position and velocity of end-effector is also fused to predict grasping representation. A key objective for fusing multimodal data is to reconstruct the raw sensor data of environmental observation.

Most of the mentioned works above fuse more than one modality data to represent the observation but only on a single scale. We can still tap the potentials not only between different modalities but different scales following [21]. Therefore, we propose our hierarchical encoder-decoder neural network to complete multi-task prediction shown in Fig 2.

III. PRELIMINARY AND PROBLEM FORMULATION

In this section, we study eye-in-hand vision based robotic grasping problem with multimodal data fusion. A parallel-jaw grasp representation [31] [7] is introduced. Comparing to other similar works, our representation contains 6D pose, orientation and gripper opening width. The object of grasping model is also proposed in this paper.

A. Grasp definition

Grasp space representation In this paper, we propose an 8D grasp representation (1) including 6D object pose $P = (x, y, z, \gamma_x, \beta_y, \alpha_z)$, gripper's orientation and opening width. Considering that we only utilize RGBD data from a single point of view, the object is partially observable and hard to achieve its precise pose estimation without sufficient prior knowledge. Therefore, we estimate grasp representation except 3D pose from the RGBD fusion algorithm and 3D pose can be obtained from the proprioception of the eye-in-hand system mentioned in V-C.

$$g = (P, \phi, w) \quad (1)$$

Transformation Grasp representation and policy generation take place in the image space and camera coordinate. The transformation ${}^{Camera}T_{Image}$ between the image space and the camera space can be calculated by intrinsic parameters of the camera. We obtain transformation from the camera space to the robot base ${}^{Robot}T_{Camera}$ by hand-eye calibration.

The RGB image with the depth image aligned to it is $I = \mathbb{R}^{4 \times H \times W}$ where H is the image height and W is the image width. We assume the intrinsic and extrinsic parameters of the camera and physics properties of the robot are known.

In the image space, the grasp representation can be rewritten as:

$$\tilde{g} = (u, v, \tilde{\phi}, \tilde{w}) \quad (2)$$

where (u, v) is the position of the grasp in the image coordination. $\tilde{\phi}$ and \tilde{w} correspond the ϕ and w in Cartesian coordinates. We can get the grasp representation in the robot base coordinates from the following the Eq. (3).

$$g = {}^{Robot}T_{Camera} \times {}^{Camera}T_{Image} \times \tilde{g} \quad (3)$$

B. Grasp labeling

The most existing grasp methods assume that the center of the target bounding box is the best grasping center point and the length and angle of the short side of the bounding box represent the gripper's best opening width and orientation. This center-based assumption is used widely in 2D and 3D bounding box.

Unlike other robotic manipulation label method using rectangles and bounding boxes, We propose a novel labeling method for the common datasets that contain RGB, depth and object's mask images. The process can be shown in Fig. 1. We also assume that the geometric center of the object is the best grasping center point as people usually grasp an object at the centroid of the object (geometric or gravity center). In addition, the shortest edge point-pair line passing the center is the best grasping instead of the bounding box's short-side direction. We use the minimum bounding box method to get a bounding box over the mask target image. This operation aims to obtain the geometric center of the target approximately. A shortest straight-line pass through two edge points and center points of the object is selected to get the gripper's opening width and orientation.

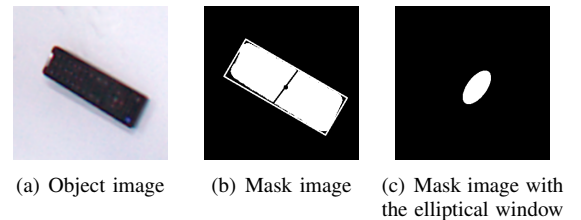


Fig. 1. Grasp Labeling Process

After obtaining the grasp representation \tilde{g} , we need to label the positive pixel area as the ground truth. Because we have only one grasp point label from the mask image, it is too sparse to train. We propose an elliptical window to label positive area as shown in Fig. 1. The elliptical window uses grasp center point as center, the shortest straight-line as long axis and half lengths as short axis. We simply believe that the area within the window has a high probability to grasp successfully and set it to 1 and also the area corresponding to width and angle image is set to the width and angle values.

C. Problem formulation

RGBD fusion grasping generation can be defined as a mapping $M : I \rightarrow G$. I indicates the RGBD image space and G is the grasping representation space which can be redefined as

$$G = (Q, \tilde{\Phi}, \tilde{W}) \quad (4)$$

where $Q, \tilde{\Phi}, \tilde{W} \in \mathbb{R}^{H \times W}$ is each pixel's probability, orientation and opening width respectively. We get the position of grasp (u, v) by selecting the pixel that has the maximum probability.

A mapping function M can be defined as:

$$G = M(I) \quad (5)$$

Our goal is to find a robust function M_θ to fit M :

$$\theta = \arg \min_{\theta} \mathcal{L}(G, M_\theta(I)) \quad (6)$$

where \mathcal{L} is the loss function between the ground truth and M_θ , θ is the parameter of function M . The optimal grasp $\tilde{g}^* = \max_Q G$ in the image space and grasp representation in robot based coordinates can be transferred via Eq. (3).

IV. THE PROPOSED METHOD

In this section, we will introduce a multimodal hierarchical encoder-decoder fully convolutional network to approximate the mapping function (5). The dataset preprocess and the loss function definition are also given. A grasping metric is proposed to evaluate our method.

A. Dataset generation and preprocessing

We use Cornell grasp detection dataset [16] and YCB Object and Model Set [32] to train our neural network. We extract a object mask image for the first one. We generate ground truth about grasping probability, gripper opening width and orientation by mask image talked in III-B.

For the orientation, we choose a gripper orientation angle ϕ in the range of $[-\frac{\pi}{2}, \frac{\pi}{2}]$ and represent $\tilde{\phi}$ as a vector $(\cos(2\tilde{\phi}), \sin(2\tilde{\phi}))$ on a unit circle of which value is a continuous distribution in $[-1, +1]$. [33] shows this processing is easy for the training. The input and output image are resized into 336×336 . We scale the depth and RGB image value between 0 and 1 by min-max normalization. The depth image is inpainted with OpenCV [34].

B. Network Design

The architecture of our neural network is named as U-Grasping network V3(UG-Net V3). In the RGB branch and depth branch, we both adopt the structure like U-Net [35] as our back-bone illustrated in Fig. 2. The last two layers of U-net is dropped and we reduce the channel of each layer to one-quarter of the original number except the input layer.

Multimodal fusion We fuse two modal feature in the decoder part of the network by a confidence net [21]. Four scale confidence maps are generated by confidence net via five convolutional layers and three max pooling layers to re-weight depth branch feature map. At last, the re-weighted

depth feature maps at four different scales are concatenated with color feature maps with the same resolution. The fusion module can be formulated as follows:

$$FM(\mathcal{F}_c^l, \mathcal{F}_d^l | \mathcal{C}^l) = \mathcal{F}_c^l \oplus (\mathcal{F}_d^l \odot \mathcal{C}^l) \quad (7)$$

where $\mathcal{F}_c^l, \mathcal{F}_d^l$ are features from RGB and depth branches at scale l . \mathcal{C}^l is the confidence map with only one channel at scale l . \oplus is the concatenate operation and \odot is the element-wise multiplication.

Background extraction module Most existing robotic grasping researches, excluding the ones using point cloud, set the camera heading vertically to the table surface, which adds a relatively strong constraint to the depth data. Since most laser-based RGBD cameras obtain 3D data by a near-infrared (NIR) pulse illumination component no matter time-of-flight or structured light, the range of depth value is simply limitless comparing to RGB data range from 0 to 255 theoretically. The existing vertical observation constrains the depth value by the table surface which makes use of depth data more easily. However, this method lets the robotic arm grasp an object like humans difficult to realize compared to utilizing 3D point cloud data to predict 6D object pose method. Therefore, to grasp without full observation and 3D prior knowledge, we propose an FCN mask network to extract the target object from the background. It is a six layer encoder-decoder neural network. We input RGB and depth image to a three-layer-encoder branch respectively and concatenate the last encoder features together and pass to the decoder block. We set the output as the object mask by a linear convolutional layers. We pretrain this mask network using YCB-dataset and then concatenate the third decoder layer to the last fusion layer shown in the top of Fig. 2 (colored in orange) by dropping the last output layer. This part enhances our method grasping performance when our observation view is not vertical to the table surface even horizontal view.

Grasping prediction We have introduced multimodal fusion and background extraction in the last two parts. In this part, we will illuminate the multi-task learning structure for the grasping representation. After concatenating the fusion features from RGB and depth branches and mask feature from Background extraction, we add three convolutional layers and one output layers to predict grasping probability, cosine value, sine value and gripper's opening width respectively. In the physical system, the depth raw data from the RGBD camera is filled with a lot of missing points. We usually process the raw depth image by inpainting. For grasping task, we not only need to process visual information to generate policy but also to obtain a real physical value not artificial to apply in the control system. Therefore, we propose an aux depth estimation output in the top left of Fig. 2. Considering the last concatenating part fusing RGB features and re-weight depth features, we believe the RGB knowledge in the fusion features can compensate poor-quality depth image features implicitly and be also used to estimate missing points in the depth image for the control

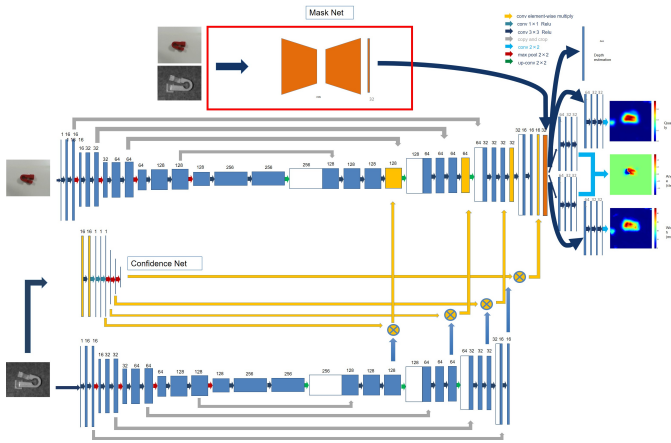


Fig. 2. **UG-Net V3 Architecture** The network contains a two-input encoder-decoder FCN network, a background extraction module, and a confidence net. We proposed an aux depth estimation to compensate poor-quality depth image. The outputs are grasping probability, cosine value, sine value and gripper’s opening width in pixel-wise respectively.

system.

C. Proposed loss function and training

Loss function For the mask network, we use mean square error loss Eq. (8) function comparing the predicted and ground-truth maps M_θ and M^* .

$$\mathcal{L}_{mask} = \frac{1}{n} \|M_\theta - M^*\|^2 \quad (8)$$

For the grasping prediction, we set the loss to:

$$\mathcal{L} = \mathcal{L}_{depth} + \mathcal{L}_{grasp} \quad (9)$$

$$\mathcal{L}_{depth}(D, D^*) = \frac{\lambda_d}{n} \sum_i d_i^2 + \frac{\lambda_d}{n} \sum_i \left[(\nabla_x d_i)^2 + (\nabla_y d_i)^2 \right] \quad (10)$$

where $d = D - D^*$, the sums are valid pixel i and n is the number of valid pixels. And the first-order matching term encourages prediction of not only close-by value but also local structure [36].

$$\begin{aligned} \mathcal{L}_{grasp} = & \frac{\lambda_q}{n} \|Q_\theta - Q^*\|^2 + \frac{\lambda_{\cos}}{n} \left\| \cos(2\tilde{\Phi})_\theta - \cos(2\tilde{\Phi})^* \right\|^2 \\ & + \frac{\lambda_{\sin}}{n} \left\| \sin(2\tilde{\Phi})_\theta - \sin(2\tilde{\Phi})^* \right\|^2 + \frac{\lambda_w}{n} \left\| \tilde{W}_\theta - \tilde{W}^* \right\|^2 \end{aligned} \quad (11)$$

where we train the gripper orientation using a vector on an unit circle talked in IV-A. We rewritten the vector $(\cos(2\tilde{\Phi}), \sin(2\tilde{\Phi}))$ and $\tilde{\Phi}$ can be computed following Eq. (12). Q^* , $\cos(2\tilde{\Phi})^*$, $\sin(2\tilde{\Phi})^*$ and \tilde{W}^* are corresponding ground-truth. λ_d , λ_q , λ_{\cos} , λ_{\sin} , λ_w are the weight coefficients and we set all of default value as 1.

$$\tilde{\Phi}_\theta = \frac{1}{2} \arctan \frac{\sin(2\tilde{\Phi})_\theta}{\cos(2\tilde{\Phi})_\theta} \quad (12)$$

Training We use 80% of the dataset for training and 20%



(a) Adversarial objects

(b) Household objects

Fig. 3. **Test Objects**

of the dataset for evaluation. The activation function for all the layers except the output layers set as *Relu* and output layers’ set as *linear*. The training of our network proceeds into two steps. In the first step, we pretrain the background extraction module firstly using YCB Object and Model Set. In the second step, we load the pretrained parameters of module except the last output layers to our main network by concatenation and we set the last decoder of the mask network trainable and fix the parameters of other layers to fine-tune the module. The Cornell grasp detection dataset is used to train the main network. We use the Adam optimizer, set batch size as 4 and train 20 epochs for both two training steps.

D. Grasping Metric

Robust grasp generation The variance of 200 times policy generation for a static observation. This evaluates the robustness of our method with various sampling noise.

Success Rate The percentage of successful grasps over all the grasp trails.

Robust Grasp Rate The ratio of probabilities higher than 50% of successful grasps through all the runs which measures the method performance from the predicted probability values.

Planning Time The time consumed between receiving the raw data and grasping policy generation output.

V. EXPERIMENT

In this section, we evaluate our method in the physical setup. We design two experiments to validate the effectiveness of our method. The first one is grasping an object with the camera view vertical to the table surface which we called grasping performance test. For another, we design a control algorithm to execute humanoid grasping operation which we called 3D grasping test.

We choose a general benchmark including 3D-printed adversarial in Dex-Net 2.0 [6] and household objects shown in Fig. 3. we also add a set of bottom-like object to validate the horizontal grasping. The final execution is taken place on a single arm Kinova Jaco 7DOF robot shown in Fig 4. We use an Intel RealSense SR300 RGBD camera to get the images mounted on the wrist of the robot. All computation is finished on a PC running Ubuntu16.04 with a Intel Core i7-8700K CPU and two NVIDIA Geforce GTX 1080ti graphic cards. It is noticed that we use two cards to accelerate the training process and just use one card to running the trained network.

A. Assumption

In our work, we assume that the intrinsic and extrinsic parameter of the camera is known. The coordinates of RGB and depth image are aligned and time stamp is synchronized. For the 3D grasping test, since we do not estimate the 6D pose of the object directly, we assume that the best grasping pose is approximately equal to the best camera viewpoint pose considering that the camera is fixed on the end-effector close to the end of gripper.

B. Grasping Performance Test

In this part, we make an analysis and comparison between the state of art methods in metrics proposed in IV-D. We also perform an ablation study to evaluate each module in our network structure.

We set up our robot as shown in Fig. 4(a). The observation height is 55 centimeters away from the table surface. We set the observation pose vertical to the table surface approximately which is the same as most of the existing works. We try to grasp each object 10 times to record the grasping results shown in TABLE I.

In the experiment, we set the network structure only containing RGB and depth encoder-decoder branch without the confidence net and background extraction module as our baseline network. All the network structure achieve a comparative high grasping success rate in the household set because some kinds of objects appeared in the training dataset. The neural network can better learn the geometric and textural features of these objects. In contrast, the result of adversarial sets shows a little poor, but the network still achieves high success rate and robust grasp rate when we adopt the additional modules which indicates the background extraction module enhances the ability of target object detection. We find that the baseline achieves 80% performance in both success rate and robust grasp rate which indicates the advantage of our fusion network structure. The confidence net is used to qualify the quality of depth image which decreases the grasping performance because of the effect of preprocessing for the training dataset and the internal differences between the sampling sensors. Although the confidence net does not achieve the best performance in table surface vertical viewpoint grasping task, it is significant in the humanoid viewpoint grasping talked in the next subsection V-C.

Apart from the ablation study, another comparison with some other state-of-the-art approaches is shown in TABLE II. Considering the difference between the used test set, we only compare the adversarial sets result used in all mentioned works. We can find our method have a desired balance between real-time and performance. Furthermore, in our work, the aux depth estimation can avoid the failure of grasping due to the depth point missing to some degree.

C. 3D Grasping Test

In this part, we evaluate our proposed method to realize a 3D grasping test. Because we use the eye-in-hand camera system that the camera is fixed very close to the end-effector,



(a) Grasping performance test

(b) 3D Grasping test

Fig. 4. Robot Setup

we assume there is a consistency between observation viewpoint and grasping pose and the best observation viewpoint is approximately equal to the best grasping pose. We propose a test set including six objects observed at 0, 22.5, 45 degree horizontal angle (pitch angle) the same with BigBIRD [37] setup shown in Fig. 4(b). We only choose the three low pitch angle setups since the other two approximate observe vertical to the table surface. The table surface guarantees the quality of depth image with less missing points while observation with low pitch angle samples less validated data because of the perception range of the sensor. The result of 3D grasping is shown in TABLE ?? . We have 10 trials for each object which is rotated along the gravity axis with a random angle and a grasp success rate is given in TABLE I.

We also try to design a grasping based on surface normal estimation to replace the grasping pose from the observation viewpoint. We set the normal vector of target grasping point align to the z-axis of camera coordinate within the shortest arc. The video can be available in

D. Pipeline

In this part, the control algorithm for the experiment is given. We set up an open-loop grasping controller to realize grasping. For the surface normal estimation, we adopt the work [38] and it takes about 470ms for each policy generation. The whole pipeline is presented in Algorithm 1.

VI. DISCUSSION

We give two experiments to evaluate the effectiveness of our network structure. In the grasping performance test V-B, we design an ablation study to validate the function of each module in our structure. From the TABLE I, we find the confidence net can constrain the depth image uncertainty strongly while the uncertainty of depth image does not be qualified directly in other works and our baseline. This property performs in the 3D grasping test V-C because the depth image is filled with abundant missing point. While the confidence net decreases the robust grasp rate, it enhances our method's robustness for different scenarios. The background extraction module splits the background and the target object to enhance the grasping policy generation especially in the complex scenario. In the 3D grasping test V-C, we assume the grasping pose keeps consistent with the camera pose in the eye-in-hand robotic system setup. The experiment result shows that only using depth and RGB

Network Structure	Baseline	Baseline Condidence Net	Baseline Background Detection	Baseline Condidence Net Background Detection
Success Rate(adversarial objects)	79±2%	73±2%	95±1%	89±1%
Robust Grasp Rate(adversarial objects)	80±1%	31±2%	97±1%	79±2%
Robust Generation(adversarial objects)	5.05	1.32	1.30	1.53
Success Rate(household objects)	96±1%	97±2%	99±1%	93±2%
Robust Grasp Rate(household objects)	97±1%	87±1%	98±2%	75±2%
Robust Generation(household objects)	1.21	3.24	3.22	3.60
Pitch angle: 0°	80±1%	64±1%	86±2%	81±1%
Pitch angle: 22.5°	80±1%	84±1%	83±2%	93±1%
Pitch angle: 45°	67±1%	90±1%	90±1%	85±1%

TABLE I

RESULTS OF THE ABLATION STUDY IN **V-B** ON THE TEST SET. DIFFERENT PITCH ANGLE GRASPING IS ALSO GIVEN MENTIONED IN **V-C**

	GQ-CNN	GG-CNN	Our baseline	Our best
Success Rate	80%	84±8%	79±2%	95±1%
Robust Grasp Rate	43%		80±1%	97±1%
Planning Time(ms)	800	19	28	32
Model Size (Approx.)	75MB	0.5MB	19.1MB	19.6MB

TABLE II

COMPARISON WITH OTHER EXISTING WORKS FROM THE METRICS PROPOSED IN **IV-D**

Algorithm 1: Hierarchical RGB-D Fused Robotic Grasp Planning

Input: RGB image I_{RGB} , depth data I_{depth}

Output: grasping g and gripper q .

```

1 while Running do
2   Preprocess  $I_{RGB}$  and  $I_{depth}$ .
3   Predict  $G$  from network  $M_\theta$ .
4   Obtain the maximum probability position  $\tilde{g}$  in pixel space.
5   if Target depth is missing then
6     Use depth estimation depth value instead.
7   Convert  $\tilde{g}$  to  $g$  according to Eq. (3).
8   if Surface normal is estimated then
9     Convert target point  $\tilde{g}$  normal vector with  $(0, 0, 1)$  into quaternion  $q$ 
10  else
11    Obtain current pose of camera view point  $q$ 
12  end
13  Approach target object with position  $g$  and pose  $q$  and close the gripper.
14 end

```

image we can also realize a 3D environment without the 6D pose estimation.

For a physical system, the real-time is needed to be considered. In our work, we compare two excellent existing works. It needs to be noticed that GQ-CNN [6] and GG-CNN [7] used GTX 1080 and GTX 1070 NVIDIA graphic card respectively. Our work adopts one GTX1080ti NVIDIA graphic card to realize grasp prediction. Although our hardware is the best of the three, it is a general capacity of calculation currently. We still believe our method has a remarkable real-time performance. Besides the surface normal based grasping is just our trial to obtain grasping pose without considering real-time too much and we can use other methods to obtain the pose such as the observation viewpoint exploration.

VII. CONCLUSIONS

In this paper, we propose a novel multimodal hierarchical neural network to realize robotic grasping in the unstructured environment. Our method only adopts partial observation by an eye-in-hand robotic arm system. Two experimental results including grasping pose vertical to the table surface and 3D humanoid grasping are given to validate the effectiveness and performance of our method. TABLE I and II indicate our grasping method achieve over 90% success rate on our test set.

However, it can still be improved in the following field. In our work, we assume the grasping pose keeps consistent with the camera pose and the best grasping pose is approximately equal to the best camera viewpoint. The gripper's pose for grasping is obtained from the camera observation pose but how to get the best observation we do not be researched in this paper. Therefore, the observation view exploration is a necessary next step. Our experiment video is available in https://youtu.be/Wxw_r5a8qV0.

REFERENCES

- [1] A. Bicchi and V. Kumar, "Robotic grasping and contact: A review," in *Proceedings 2000 ICRA. Millennium Conference. IEEE International Conference on Robotics and Automation. Symposia Proceedings (Cat. No. 00CH37065)*, vol. 1, pp. 348–353, IEEE, 2000.

- [2] M. Mason, "The mechanics of manipulation," in *Proceedings. 1985 IEEE International Conference on Robotics and Automation*, vol. 2, pp. 544–548, IEEE, 1985.
- [3] T. Lozano-Pérez, "Motion planning and the design of orienting devices for vibratory part feeders," in *IEEE Journal Of Robotics And Automation. MIT AI Laboratory*, 1986.
- [4] M. Schwarz, A. Milan, C. Lenz, A. Munoz, A. S. Periyasamy, M. Schreiber, S. Schüller, and S. Behnke, "Nimbro picking: Versatile part handling for warehouse automation," in *2017 IEEE International Conference on Robotics and Automation (ICRA)*, pp. 3032–3039, IEEE, 2017.
- [5] A. Zeng, K.-T. Yu, S. Song, D. Suo, E. Walker, A. Rodriguez, and J. Xiao, "Multi-view self-supervised deep learning for 6d pose estimation in the amazon picking challenge," in *2017 IEEE International Conference on Robotics and Automation (ICRA)*, pp. 1386–1383, IEEE, 2017.
- [6] J. Mahler, J. Liang, S. Niyaz, M. Laskey, R. Doan, X. Liu, J. A. Ojea, and K. Goldberg, "Dex-net 2.0: Deep learning to plan robust grasps with synthetic point clouds and analytic grasp metrics," *Robotics: Science and Systems (RSS)*, 2017.
- [7] D. Morrison, P. Corke, and J. Leitner, "Closing the loop for robotic grasping: A real-time, generative grasp synthesis approach," *arXiv preprint arXiv:1804.05172*, 2018.
- [8] A. Zeng, S. Song, S. Welker, J. Lee, A. Rodriguez, and T. Funkhouser, "Learning synergies between pushing and grasping with self-supervised deep reinforcement learning," in *2018 IEEE/RSJ International Conference on Intelligent Robots and Systems (IROS)*, pp. 4238–4245, IEEE, 2018.
- [9] G. Thomas, M. Chien, A. Tamar, J. A. Ojea, and P. Abbeel, "Learning robotic assembly from cad," in *2018 IEEE International Conference on Robotics and Automation (ICRA)*, pp. 1–9, IEEE, 2018.
- [10] R. M. Murray, *A mathematical introduction to robotic manipulation*. CRC press, 2017.
- [11] B. Siciliano and O. Khatib, *Springer handbook of robotics*. Springer, 2016.
- [12] B. Kehoe, A. Matsukawa, S. Candido, J. Kuffner, and K. Goldberg, "Cloud-based robot grasping with the google object recognition engine," in *2013 IEEE International Conference on Robotics and Automation*, pp. 4263–4270, IEEE, 2013.
- [13] J. Weisz and P. K. Allen, "Pose error robust grasping from contact wrench space metrics," in *2012 IEEE international conference on robotics and automation*, pp. 557–562, IEEE, 2012.
- [14] J. Bohg, A. Morales, T. Asfour, and D. Kragic, "Data-driven grasp synthesis survey," *IEEE Transactions on Robotics*, vol. 30, no. 2, pp. 289–309, 2013.
- [15] R. Detry, C. H. Ek, M. Madry, and D. Kragic, "Learning a dictionary of prototypical grasp-predicting parts from grasping experience," in *Robotics and Automation (ICRA), 2013 IEEE International Conference on*, pp. 601–608, IEEE, 2013.
- [16] I. Lenz, H. Lee, and A. Saxena, "Deep learning for detecting robotic grasps," *The International Journal of Robotics Research*, vol. 34, no. 4-5, pp. 705–724, 2015.
- [17] D. Kappler, J. Bohg, and S. Schaal, "Leveraging big data for grasp planning," in *Robotics and Automation (ICRA), 2015 IEEE International Conference on*, pp. 4304–4311, IEEE, 2015.
- [18] R. Balasubramanian, L. Xu, P. D. Brook, J. R. Smith, and Y. Matsuoka, "Physical human interactive guidance: Identifying grasping principles from human-planned grasps," *IEEE Transactions on Robotics*, vol. 28, no. 4, pp. 899–910, 2012.
- [19] S. Levine, P. Pastor, A. Krizhevsky, J. Ibarz, and D. Quillen, "Learning hand-eye coordination for robotic grasping with deep learning and large-scale data collection," *The International Journal of Robotics Research*, vol. 37, no. 4-5, pp. 421–436, 2018.
- [20] F. Sadeghi, A. Toshev, E. Jang, and S. Levine, "Sim2real viewpoint invariant visual servoing by recurrent control," in *Proceedings of the IEEE Conference on Computer Vision and Pattern Recognition*, pp. 4691–4699, 2018.
- [21] J. Zeng, Y. Tong, Y. Huang, Q. Yan, W. Sun, J. Chen, and Y. Wang, "Deep surface normal estimation with hierarchical rgb-d fusion," in *Proceedings of the IEEE Conference on Computer Vision and Pattern Recognition*, pp. 6153–6162, 2019.
- [22] E. Arruda, J. Wyatt, and M. Kopicki, "Active vision for dexterous grasping of novel objects," in *Intelligent Robots and Systems (IROS), 2016 IEEE/RSJ International Conference on*, pp. 2881–2888, IEEE, 2016.
- [23] A. T. Pas, M. Gualtieri, K. Saenko, and R. Platt, "Grasp pose detection in point clouds," *International Journal of Robotics Research*, vol. 36, no. 13, p. 027836491773559, 2017.
- [24] J. Sung, J. K. Salisbury, and A. Saxena, "Learning to represent haptic feedback for partially-observable tasks," in *2017 IEEE International Conference on Robotics and Automation (ICRA)*, pp. 2802–2809, IEEE, 2017.
- [25] G.-H. Liu, A. Siravuru, S. Prabhakar, M. Veloso, and G. Kantor, "Learning end-to-end multimodal sensor policies for autonomous navigation," *arXiv preprint arXiv:1705.10422*, 2017.
- [26] Y. Bekiroglu, R. Detry, and D. Kragic, "Learning tactile characterizations of object-and pose-specific grasps," in *2011 IEEE/RSJ International conference on Intelligent Robots and Systems*, pp. 1554–1560, IEEE, 2011.
- [27] R. Calandra, A. Owens, D. Jayaraman, J. Lin, W. Yuan, J. Malik, E. H. Adelson, and S. Levine, "More than a feeling: Learning to grasp and regrasp using vision and touch," *IEEE Robotics and Automation Letters*, vol. 3, no. 4, pp. 3300–3307, 2018.
- [28] Y. Gao, L. A. Hendricks, K. J. Kuchenbecker, and T. Darrell, "Deep learning for tactile understanding from visual and haptic data," in *2016 IEEE International Conference on Robotics and Automation (ICRA)*, pp. 536–543, IEEE, 2016.
- [29] J. Sinapov, C. Schenck, and A. Stoytchev, "Learning relational object categories using behavioral exploration and multimodal perception," in *2014 IEEE International Conference on Robotics and Automation (ICRA)*, pp. 5691–5698, IEEE, 2014.
- [30] M. A. Lee, Y. Zhu, K. Srinivasan, P. Shah, S. Savarese, L. Fei-Fei, A. Garg, and J. Bohg, "Making sense of vision and touch: Self-supervised learning of multimodal representations for contact-rich tasks," in *2019 International Conference on Robotics and Automation (ICRA)*, pp. 8943–8950, IEEE, 2019.
- [31] Y. Jiang, S. Moseson, and A. Saxena, "Efficient grasping from rgb-d images: Learning using a new rectangle representation," in *2011 IEEE International Conference on Robotics and Automation*, pp. 3304–3311, IEEE, 2011.
- [32] B. Calli, A. Walsman, A. Singh, S. Srinivasa, P. Abbeel, and A. M. Dollar, "Benchmarking in manipulation research: Using the yale-cmu-berkeley object and model set," *IEEE Robotics & Automation Magazine*, vol. 22, no. 3, pp. 36–52, 2015.
- [33] K. Hara, R. Vemulapalli, and R. Chellappa, "Designing deep convolutional neural networks for continuous object orientation estimation," *arXiv preprint arXiv:1702.01499*, 2017.
- [34] G. Bradski and A. Kaehler, "Opencv," *Dr. Dobbs journal of software tools*, vol. 3, 2000.
- [35] O. Ronneberger, P. Fischer, and T. Brox, "U-net: Convolutional networks for biomedical image segmentation," in *International Conference on Medical image computing and computer-assisted intervention*, pp. 234–241, Springer, 2015.
- [36] D. Eigen and R. Fergus, "Predicting depth, surface normals and semantic labels with a common multi-scale convolutional architecture," in *Proceedings of the IEEE international conference on computer vision*, pp. 2650–2658, 2015.
- [37] A. Singh, J. Sha, K. S. Narayan, T. Achim, and P. Abbeel, "Bigbird: A large-scale 3d database of object instances," in *2014 IEEE International Conference on Robotics and Automation (ICRA)*, pp. 509–516, IEEE, 2014.
- [38] X. Qi, R. Liao, Z. Liu, R. Urtasun, and J. Jia, "Geonet: Geometric neural network for joint depth and surface normal estimation," in *Proceedings of the IEEE Conference on Computer Vision and Pattern Recognition*, pp. 283–291, 2018.